ADVANCED FUNCTIONAL MATERIALS
www.afm-journal.de

The Magnetohydrodynamic Effect and Its Associated Material Designs for Biomedical Applications: A State-of-the-Art Review

*Thomas Stanley Gregory, Rui Cheng, Guoyi Tang, Leidong Mao, and Zion Tsz Ho Tse**

The presented article discusses recent advances in biomedical applications of classical magnetohydrodynamics (MHD), with a focus on operating principles and associated material considerations. These applications address novel approaches to common biomedical problems from microparticle sorting for lab-on-a-chip devices to advanced physiological monitoring techniques. 100 papers in the field of MHDs are reviewed with a focus on studies with direct biomedical applications. The body of literature is categorized into three primary areas of research including material considerations for MHD applications, MHD actuation devices, and MHD sensing techniques. The state of the art in the field is examined and research topics are connected to provide a wide view of the field of biomedical MHDs. As this field develops, the need for advanced simulation and material design will continue to increase in importance in order to further expand its reach to maturity. As the field of biomedical MHDs continues to grow, advances toward microscale transitions will continue to be made, maintaining its clinically driven nature and moving toward real-world applications.

1. Introduction

The magnetohydrodynamic (MHD) effect is a physical phenomenon describing the motion of a conducting fluid flowing under the influence of an external magnetic field. Its applications have been studied extensively across multiple disciples ranging from the study of solar winds[1,2] to MHD-derived biomedical sensors[3] and actuators.[4–7] Despite this research, alternative uses of the MHD effect are emerging topics, particularly those of clinical significance or addressing biomedical problems.

The field of MHDs with a focus on studies with direct biomedical applications was surveyed, and literature that helps to advance the current state of the art was reviewed and presented in this body of work. The research was introduced through a theoretical presentation of the underlying physics followed by three primary research areas: (1) macro- and microscale theoretical magnetohydrodynamics; (2) material considerations for MHD applications; (3) MHD actuation devices; and (4) MHD sensing techniques. These research topics focus on macro- and microscale treatments, with applications being considered in the field of magnetic resonance imaging (MRI), microfluidics and analytical chemistry, and guided drug delivery among others.

It is the aim of this paper to present the current state of the literature with regards to clinical applications of the MHD effect, and outline predictions for the further growth and development of the field.

T. S. Gregory, R. Cheng, Prof. L. Mao, Prof. Z. T. H. Tse
College of Engineering
The University of Georgia
597 D.W. Brooks Drive, Athens, GA 30602, USA
E-mail: ziontse@uga.edu
Prof. G. Tang
Advanced Materials Institute
Graduate School at Shenzhen
Tsinghua University
Shenzhen 518055, P.R. China

DOI: 10.1002/adfm.201504198

2. Theory

The study of the MHD effect involves the coupling of electromagnetism, specifically regarding induction, to dynamics. This coupling is necessary when the material in question can behave as a conductor and through this have the ability to modify and be modified by the external magnetic fields when there is relative motion, creating a dominant physical force in conductive fluids with high volumetric flow rates and in large current carriers. The magnitude and direction of the fluid flow ($\vec{v}$) and the magnetic field ($\vec{B_o}$) both directly affect the magnitude and resultant direction of the MHD effect, creating a variance in induced Hall effect voltages.[8] The following is a presentation of MHD theory through the derivation of Maxwell's equations coupled with fluid flow. **Table 1** lists a table of terms used in this derivation.

2.1. Electromagnetism

The basis of the MHD effect must first be examined in terms of the primary magnetic field ($\vec{B_o}$), and Maxwell's equations (Equations (1)–(4)) expressed in differential form to predict the

Table 1. Terms used in derivation of MHD underlying physics.

Term	Description	Units
$\vec{v}$	Magnitude and direction of fluid flow	mL s^{-1}
L	Length of fluid flow field	M
$\vec{B}_o$	Magnitude and direction of the applied magnetic field	T, G
E	Electric field	N C^{-1}, V m^{-1}
ρ_e	Charge density	C m^{-2}
J	Current density	A m^{-2}
ε_o	Permittivity of free space	F m^{-1}
μ_o	Permeability of free space	H m^{-1}, N A^{-2}
μ	Magnetic permeability	H m^{-1}, N A^{-2}
c	Magnetic susceptibility	–
σ	Material conductivity	S m^{-1}
η	Magnetic diffusivity	mA^2 W N^{-1}
Re_m	Magnetic Reynold's number	–
Q	Flow rate	m^3 s^{-1}
ρ_{fluid}	Fluid density	kg m^{-3}
μ_V	Coefficient of fluid viscosity	m^2 s^{-1}
p	Fluid pressure	N m^{-2}
f_{EM}	External applied forces	N
f_L	Lorentz force	N
f_{VB}	Magnetophoretic force	N
f_E	Electrostatic force	N

interactions between magnetic fields and electric fields, currents, and charges

$$\nabla \cdot \vec{E} = \frac{\rho_e}{\varepsilon_o} \tag{1}$$

$$\nabla \cdot \vec{B} = 0 \tag{2}$$

$$\nabla \times \vec{E} = -\frac{\partial \vec{B}}{\partial t} \tag{3}$$

$$\nabla \times \vec{B} = \mu_0 \left(\vec{J} + \varepsilon_0 \frac{\partial \vec{E}}{\partial t} \right) \tag{4}$$

Assuming that the medium is highly conductive (such as in blood flow,[9] the displacement current becomes negligible as the propagation of electric fields is inhibited. This allows Equation (4) to be further simplified to remove the displacement current (second parenthetical term). In order to define this phenomenon in terms of the external magnetic field, Ohm's law must be employed (Equation (5)) and further modified to include induction (Equation (6))

$$J = \sigma E \tag{5}$$

$$\vec{J} = \sigma \left(\vec{E} + \vec{v} \times \vec{B} \right) \tag{6}$$

Leidong Mao is an Associate Professor in the College of Engineering at the University of Georgia. He received his B.S. degree in Materials Science from Fudan University, Shanghai, China, in 2001. He received his Master of Science degree, and Doctor of Philosophy degree in Electrical Engineering from Yale University, New Haven, CT, in 2002 and 2007, respectively. His current research interests include magnetic liquids and its application in biomedical applications such as cell sorting and single cell study. He received the NSF Career Award in 2012 and a Young Scientist Award from International Conference of Magnetic Fluids in 2013.

Zion Tsz Ho Tse received his Ph.D. in Mechatronics in Medicine from Imperial College London. Currently he is an assistant professor in the College of Engineering and the Principal Investigator of the Medical Robotics Lab at the University of Georgia, Athens, GA, USA. Before joining UGA, he was a research fellow at Harvard Medical School and Brigham and Women's Hospital. Dr. Tse has been involved in designing and prototyping a broad range of novel analog-digital electronic devices, most of which have been applied in numerous clinical and industrial environments.

In such a situation where a current is allowed to flow across the medium, an additional force is present (the Lorentz force) due to the interaction between the external magnetic field and that of the conductor (Equation (7)). Equation (3) can be substituted into Equation (7) to yield a more relevant version of the Lorentz force (Equation (8))

$$\vec{F} = \vec{J} \times \vec{B} \tag{7}$$

$$F = \left(\frac{1}{\mu_o} \right) (\nabla \times \vec{B}) \times \vec{B} \tag{8}$$

Through the derivation of the behavior of interacting magnetic fields, Maxwell's equations can then be applied to fluid flow and MHDs.

Adv. Funct. Mater. **2015**,
DOI: 10.1002/adfm.201504198

2.2. Application to Fluid Flow

In order to fully describe the behavior of a flowing fluid in the presence of an external magnetic field, first consider a fluid channel under normal conditions and then subject it to an external applied force. The Navier–Stokes equation for an incompressible Newtonian fluid flowing through a pipe (Equation (9)) provides a simple solution for the system under applied external electromagnetic body forces in this case

$$\rho\left(\frac{\partial\vec{v}}{\partial t}+\vec{v}\,.\,\nabla\vec{v}\right)=-\nabla p+\mu_{\mathrm{V}}\nabla^{2}\vec{v}+ \tag{9}$$

When considering the flowing molten metal or blood within the human body under the exposure to an applied magnetic field, microscale particulate interactions must be considered due to variances in compositions. As these solutions are typically considered well-mixed, homogeneous solutions, the bulk of flow can be considered nearly electrically neutral, and the total electromagnetic force can be expressed as a summation of Lorentz, magnetophoretic (occurring in ferrous materials), and electrostatic forces[10–13] (Equation (10))

$$\vec{f}_{\mathrm{EM}}=\vec{f}_{\mathrm{L}}+\vec{f}_{\mathrm{VB}}+\vec{f}_{\mathrm{E}} \tag{10}$$

During the consideration of most clinical applications of the MHD effect, the applied magnetic field is uniform and static, especially during MRI, and magnetophoretic and electrostatic forces become null in Equation (10).[11] This simplification in this special case, allows for the only remaining force, the Lorentz force (Equation (8)) to be substituted into the Navier–Stokes equation (Equation (11)). This describes the flow of a conductive fluid when subjected to an external magnetic field

$$\rho\left(\frac{\partial\vec{v}}{\partial t}+\vec{v}\cdot\nabla\vec{v}\right)=-\nabla p+\mu_{\mathrm{V}}\nabla^{2}\vec{v}+\left(\frac{1}{\mu_{\mathrm{o}}}\right)\left(\nabla\times\vec{B}\right)\times\vec{B} \tag{11}$$

2.3. Scaling Effect and Dimensionless Number

Scaling effects in MHDs are important consideration in biomedical applications. MHD affects flows in channels that can vary from 10^{-6} to 10^{-2} m in width.[14] Nguyen summarized basic dimensionless numbers for scaling the traditional MHD model down to this range.[15] For example, the magnetic Reynolds number characterizes magnetic advection to the magnetic diffusion (Equation (12))[16]

$$Re_{\mathrm{m}}=\frac{vl}{\eta},\ \eta=\frac{1}{\mu\sigma} \tag{12}$$

In traditional MHD systems, such as the sun, its flow field has strong interaction with the magnetic field, as a result, the magnetic Reynolds number is very large.[17] However, for a typical scale (10^{-6}–10^{-2} m) and a velocity (10^{-4}–10^{-1} m s^{-1}) in biomedical flows, the upper limit of magnetic Reynolds number is on the order of 10^{-2}.[18] (Here, the magnetic diffusivity is selected as 1 m^2 s^{-1}.[15] Therefore, advection effect is not important in biomedical flows. Another two dimensionless numbers comparing the Lorentz force against the fraction force and the inertial force are the Hartmann number (*Ha*)[16]

$$Ha=\frac{\text{Lorentz force}}{\text{Friction force}}=Bl\sqrt{\frac{\sigma}{\mu_{\mathrm{V}}}} \tag{13}$$

and the interaction number *N*[16]

$$N=\frac{\text{Lorentz force}}{\text{Inertial force}}=\frac{\sigma B^{2}l}{\rho_{\mathrm{fluid}}\nu} \tag{14}$$

Both numbers decrease linearly as the dimension of the system decreases, which suggests Lorentz force does not benefit from miniaturization, and a larger magnetic field flux density may be needed for pronounced MHD effects. Finally, the governing equation for MHD (Equation (11)) at microscale becomes

$$0=-\nabla p+\mu_{\mathrm{V}}\nabla^{2}\vec{v}+\vec{J}\times\vec{B} \tag{15}$$

3. Material Considerations for MHD Applications

In order to harness the MHD phenomena in real-world applications, such as chemical mixing and physiological monitoring, several basic materials considerations must be examined. These applications become of a particular importance when dealing with very strong external magnetic fields, such as the 1.5 or 3 T magnetic field employed by the majority of MRI scanners, and when interacting with biological tissue. These considerations are primarily twofold and involve the selection of materials to maintain: (1) a desired level of functionality within a strong external magnetic field; and (2) a level of biocompatibility in which negative interactions with biological tissues do not occur over time. An overview of these considerations in presented in **Table 2**.

3.1. External Magnetic Field Exposure

As previously mentioned, several external electromagnetic forces may interact with constituent system materials when reduced to the microscale. In the case of ferrous materials, an external magnetophoretic force becomes significant and can adversely affect predicted results and proper chemical mixing in MHD driven systems. As the strength of the magnetic field increases, it may produce high applied forces and torques on ferromagnetic or highly paramagnetic materials introduced into the field, offsetting applied MHD forces.[19–21] Furthermore, in the case of microscale applications, any inhomogeneity in the external magnetic field may reduce method accuracy, which drives the need for the removal of ferromagnetic and highly paramagnetic materials in the design and construction of MHD actuators.

When selecting materials in these environments, first and foremost, magnetic susceptibility (c) must be examined, the

Table 2. Overview of biocompatible MHD material considerations.

Material	Magnetic susceptibility (c)	Electrical conductivity [S cm^{-1}]	Typical applications	ref.
Nylon	Diamagnetic $c < 0$	10^{-13}	Drug delivery devices, skin/cartilage	[87,88]
PTFE		10^{-19}–10^{-18}		
Wood		10^{-14}–10^{-4}	N/A	
Copper		6×10^{7}	Biosensors, electrodes	[89]
Dacron		10^{-25}–10^{-23}	Cardiovascular prostheses	[90–92]
Teflon		10^{-25}–10^{-23}		
Silicone (hard rubber)		10^{-14}	Artificial organ replacement	[93–95]
Cellulose		10^{-13}		
Aluminum (Al_2O_3)	Paramagnetic $0 < c < 1$	2.5×10^{6}	Dental implants	
Platinum		9.4×10^{6}	Biosensors, electrodes	[96–98]
Magnesium (WE43)		6.7×10^{6}	Cardiovascular prostheses	[99,100]
Titanium		$5–7 \times 10^{6}$	Skeletal or joint implants	[28,29,33]
Cp-Ti		$5–7 \times 10^{6}$		
Ti-5Al-2.5Fe		$5–7 \times 10^{6}$		
Ti-6Al-7Nb		$5–7 \times 10^{6}$		
Ti-6Al-4V		$5–7 \times 10^{6}$	Skeletal implants	
Stainless steel	Ferromagnetic $c > 1$	1.45×10^{6}	Skeletal implants	[28,29,33]

measure of a material's tendency to interact with an external magnetic field and offset its desired value.[22] The choice of material magnetic susceptibility in these applications, particularly in high-field MRI applications, must be either diamagnetic ($c < 0$), or slightly paramagnetic ($0 < c < 0.1$).[22] Highly desirable materials to prevent interactions with the MHD effect, and produce solely an applied Lorentz force, are typically nylon, PTFE, wood, copper, aluminum (Al), titanium (Ti), ceramics, and the majority of engineering plastics.[23] Higher paramagnetic metals such as Al and Ti may produce an image artifact in MRI applications, but are generally safe for use in commercial MHD actuators and mixers.[22]

During pulsed or rapid magnetic field gradient ramps, material conductivity is also an important factor to consider, especially in human-device interactions, due to induced heating and eddy currents.[22] Conventionally, human-device interactions for bio-sensing are performed using nonferrous conducting electrodes, and may be capacitively coupled to patient tissue through the layering of conductive and nonconductive materials.[24] In either case, they are typically isolated using RF filters designed to divert RF energy from the test electrode, and are externally interfaced to with carbon lead clips and high-impedance cabling.[24,25]

As the local magnetic field strength decreases, these potential material selection issues become less of a concern, but must be accounted for during the design stages. Furthermore, the careful control of the applied magnetic field can yield the ability to place ferromagnetic materials in magnetic fringe fields, such as in the case of ferrous conducting rods or electrodes designed to produce an electric field across a magnetic field.

3.2. Biocompatible Materials and Implants

In the case of medical applications of the MHD effect, several issues in biocompatibility must be addressed, and only nonviable materials should be chosen for implantation or interaction with biological tissue.[26] Common biomaterials selected for implantable medical devices are dependent on the human body application, and may involve: (1) Ti or Ti alloys for skeletal or joint replacements; (2) Ti alloys, Dacron, Teflon, or similar engineering plastics for cardiovascular or blood vessel prostheses; (3) polyurethane, silicone rubber, silicone, or cellulose for artificial organ replacement; and (4) hydrogels, collagen, or platinum electrodes for sensing and ocular devices.[27]

As Ti and Ti alloys maintain a relatively low magnetic susceptibility, serving as a mid-level paramagnetic material, they are often suitable for both implantable medical devices and operation within an external magnetic field. Ti alloys have conventionally been used in biomedical implants since the early 1970s, with their accepted forms and material specifications described in ASTM and ISO 5832 standards.[28] The use of Ti alloys as biomaterials increased due to their reduced elastic modulus, superior biocompatibility, high strength to weight ratio, and enhanced corrosion resistance when compared to conventional stainless steel and Co-Cr alloys.[29] The CP-Ti and Ti-6Al-4V alloys are the most common in medical applications, with CP-Ti being favored due to its surface properties which result in the spontaneous build-up of a stable and inert oxide layer.[30,31]

Due to its poor wear resistance, the Ti-6Al-4V is not suitable for bearing surface applications such as hip heads and femoral

Adv. Funct. Mater. **2015**,
DOI: 10.1002/adfm.201504198

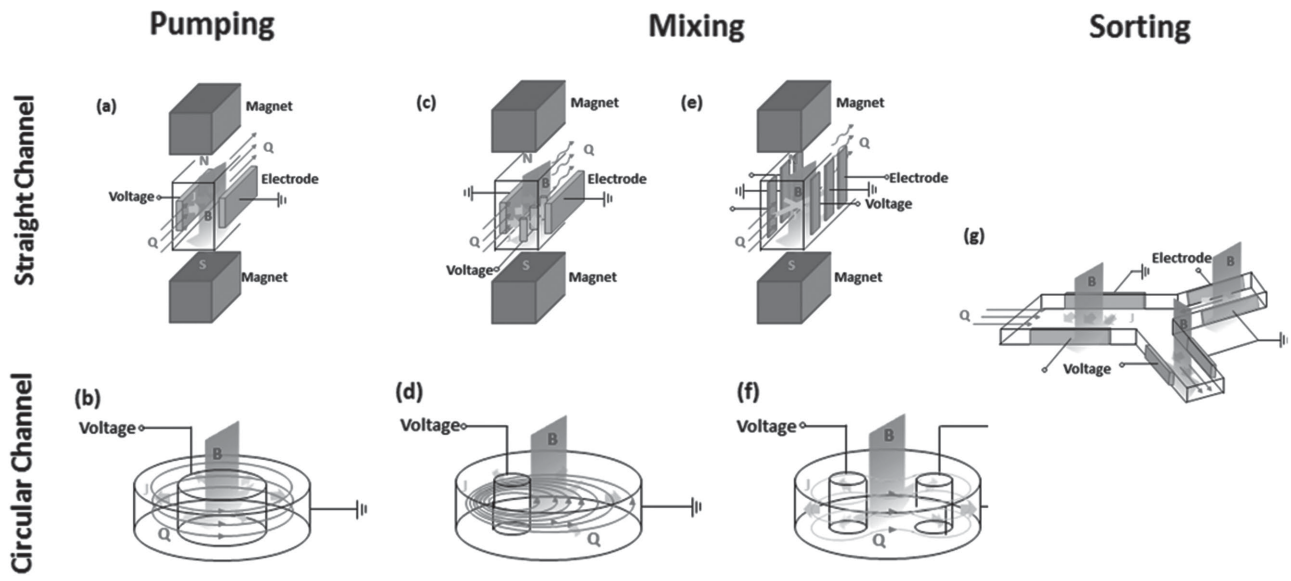

Figure 1. MHD based microflow manipulations: a) DC operated micropumps in a straight channel and b) a circular channel; c,e) AC operated micromixer in straight channels and d,f) circular chambers; and g) MHD micropump based sorting device. Images are reproduced from refs. [14,24,25,27,30] and [31].

knees, without a coating or surface treatment, and furthermore Vanadium (V) and Al elements have been shown to be toxic to the human body, resulting in the development of β alloys free of V such as Ti-6Al-7Nb and Ti-5Al-2.5Fe, which yields better biocompatibility as well as additional advantages over Ti-6Al-4V such as higher fatigue strength and lower elastic modulus.[32–34]

Through the presented advantages of these Ti alloys as a biomaterial, and the paramagnetic characterization of some of these Ti alloys, Ti presents itself as a highly favorable material for the development of biocompatible medical devices, and in the case of medical devices and applications driven by the MHD effect in which strength is a key design factor.

4. MHD Actuation Devices

Since the discovery of the MHD effect, efforts have been made toward scaling it down to microscale and applying it in a variety of areas. Among them, MHD based micropumps, micromixers, particle and cell manipulation were developed. We will review these applications.

4.1. MHD Micropumps

MHD micropumps were developed with a goal of applying them in applications such as drug delivery and lab-on-a-chip polymerase chain reaction (PCR).[4] In a typical setup, MHD micropump drives conductive liquid through an applied Lorentz force, which can be exerted onto the liquid without any mechanical moving parts. As a result, MHD micropumps possess a much simpler structure and fabrication process when compared to their mechanical counterparts. Both direct current (DC) and alternate current (AC) MHD micropumps have been developed. **Figure 1**a shows a typical drawing of an MHD micropump, including an electrode pair and permanent magnets. The flowing direction of the liquid can be controlled via the direction of the current and magnetic field. Continuous flow devices using circular microchannels and driven by AC MHD (Figure 1b) were also developed for thermal cycling PCR.[35]

In order to use MHD micropumps for drug delivery, stability of the flow rate is critical. Flow rate of MHD micropumps depends on the current density and the magnetic flux density.[4] Since the flux density from a permanent magnet is much larger than that of an electromagnet, a DC MHD pump can achieve higher flow rates than its AC counterpart, however, the problem with DC pumps is that hydrolysis often occurs during their operation, which generates bubbles and leads to electrode corrosion. Bubble generation is a serious issue, as bubbles formed on the electrode surface can isolate the electrodes from conductive solutions, which may deteriorate the pump or even result in total failure.[11] Bubbles can also obstruct flows and create instabilities for drug delivery.[36]

There are several approaches in solving the bubble problem in MHD pumps. First, bubble generation is less of a problem in AC MHD micropumps.[37] Second, one can create additional chambers for bubble releasing and trapping, in order to reduce the bubble generation and still take advantages of the high current density associated with DC pumps.[38,39] Third, redox electrolyte pairs and inert electrodes can be used to minimize bubble generation.[40]

4.2. MHD Micromixers

Rapid and efficient mixing is critical to most microfluidic systems because many biological processes—such as DNA

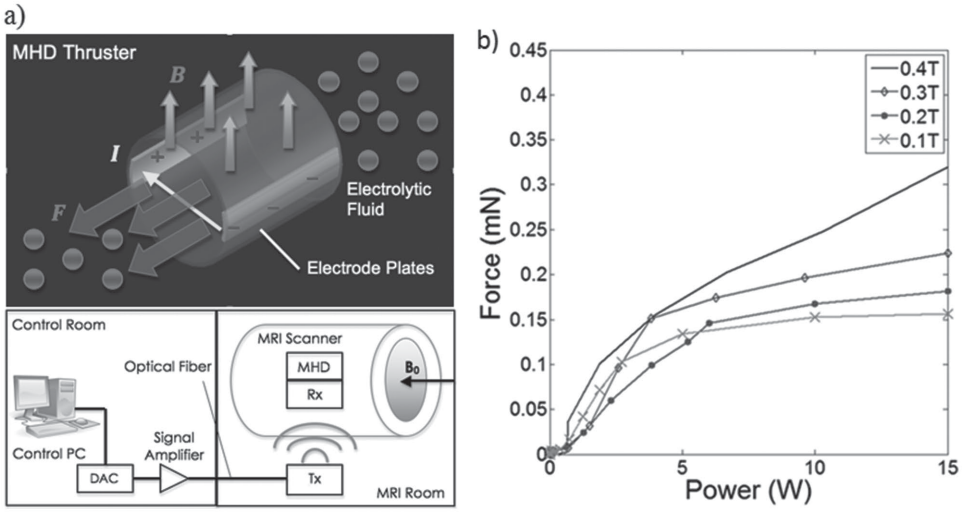

Figure 2. Development of an MRI-compatible magnetohydrodynamically driven endocapsule. a) Translation of the MHD effect into a source of propulsion (top), and the design of an MHD thruster for use in an MRI scanner (bottom). b) Quantification of system dynamic performance; step input response.

hybridization, cell activation, enzyme reactions, and protein synthesis—require rapid reactions that inevitably require efficient mixing of these reagents.[41–43] Typically, biological reagents have relatively low diffusion coefficients; for a diffusion-based device, the mixing process can take on the order of tens of seconds or minutes. This is particularly true when the solution contains macromolecules (e.g., DNA and proteins) or large particles (e.g., bacteria and blood cells) that have diffusion coefficients orders of magnitude lower than that of most small molecules. For this purpose, MHD micromixers were developed.

Typically, MHD mixers use Lorentz force exerted on electrolyte solutions in order to generate complex flow and achieve mixing. When electrodes are configured to induce recirculation in the electrolyte, complex flows can be created to enhance mixing in the channel. The patterns of complex flow depend on the electrode configuration; two of such designs are shown in Figure 1c,e.[44] In other designs, chaotic advections were induced in circular cavities, as shown in Figure 1d,f.[45] Such complex flow and chaotic advection greatly enhance the mass transport of reagents. MHD mixers have also been integrated with an axial flow so that the mixing process was accomplished along with fluid transport.[46] MHD pumps and mixers could be integrated within one device,[47] or to form complex fluidic networks.[10]

4.3. Other Microscale MHD Devices and Applications

An MHD based microfluidic switcher was developed and shown in Figure 1g.[48] In this design, two AC MHD micropumps were integrated into the arms of a Y-shape channel. As a result, flow can be switched from one arm to the other very quickly. This opens the door to device design that can control on-chip assays. One of such assays is cell sorting, which was also demonstrated via mouse neural stem cells and neuroblastoma cells by the same group.[49]

4.4. Remote Drug Delivery

The development of the MHD effect as a propulsive force, further allows for the design of advanced surgical microrobots, taking advantage of the strong magnetic field of the MRI and inherent RF capabilities, further allowing for remote navigation and control during imaging using wireless power transfer schemas (**Figure 2**a).[50] This device was shown to generate a peak force of 0.31 mN (Figure 2b), derived based on the microscale considerations presented and the unique potential for MRI-compatible devices to harness the strong magnetic field of the MRI scanner, which is typically 1.5 to 3 T in magnitude, allowing for large increases in the Lorentz body force applied to the capsule as compared to the much lower field strengths in similar medical applications of the MHD effect.

Material electrodes must be constructed from either redox pairs, such as $FeCl_2/FeCl_3$, or corrosion resistant titanium, which maintains a high level of biocompatibility and is easily sterilized. The outer capsule must serve to isolate the capsule from the body, without impairing body function. Polycarbonate materials are often utilized for this, due to their accepted usage in the development of medical instruments,[51,52] and their ease of use in modern rapid-prototyping technologies.[53,54] This application of the Lorentz force as a propulsor in the environment of an MRI scanner, illustrates comparable body forces to similarly designed devices with alternate methods of propulsion, and demonstrating the device ability to operate remotely and its potential for remote drug delivery.[55–57]

5. MHD Sensing Techniques

In addition to macro- and microscale actuation techniques that have been presented, a field of MHD sensing has also emerged, using an external magnetic field to quantify fluid flow for the applications of mechanical rate sensing,[3,58–60] hemodynamic monitoring,[61] and advanced feedback control.[62]

DOI: 10.1002/adfm.201504198

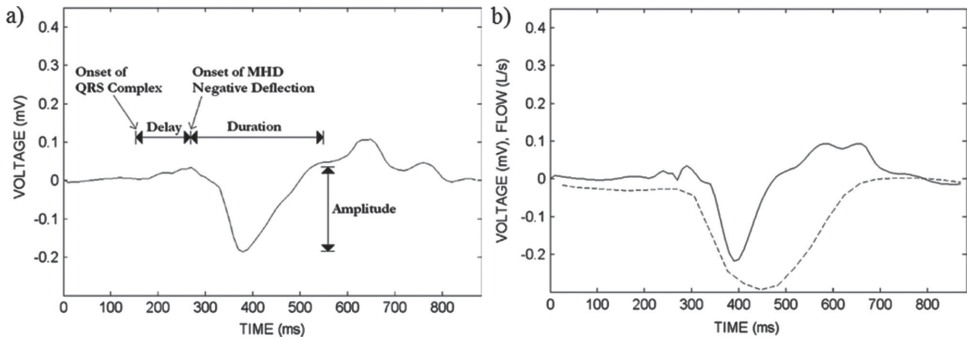

Figure 3. Correlation between induced VMHD in intra-MRI ECG recordings and MRI-derived aortic blood flow, illustrating temporal alignment. a) Extracted VMHD with measurements of duration of MHD negative deflection and delay from QRS complex. b) Extracted MHD signal (solid line) and MRI flow (dashed line) with the subject in the supine position.

5.1. Mechanical Rate and Fluid Flow Sensing

Due to the physical scale of modern hardware employed in MHD-enabled actuators, the ability to develop compact sensing platforms based on this technology became an apparent goal. Early work included the development of MHD angular rate sensors to quantify angular velocity, based on a small circular channel filled with a conductive fluid.[3,59] An external electromagnetic winding or a static magnet is configured perpendicular to the flow direction, and responsible for induced MHD interactions. In response to the rotation of the device within the magnetic field, a circumferential fluid velocity is produced and an external signal is generated which can be measured by complementary electrode pairs or a pick-up coil.[63–65] The resultant signal produces a measure of angular velocity, and can be employed easily with a static magnet without an external power source. These sensors are commonly applied when the need to correct/quantify low level vibrations [66] or high angular rates.[63]

During modern metallurgic processes, such as the manufacture of high quality steels, high accuracy velocity and flow measurements of molten metal are necessary metrics for effective quality control.[67] In the case of flowing molten metal, magnetic probes are often used to induce MHD signals, and directly quantify flow at each stage in the manufacturing process.[67–70]

5.2. Human Body Hemodynamic Sensing

As the study of MHD sensing applications continues to grow, additional efforts in flow sensing were applied to the human body, with early observations of the MHD effect being made in the strong magnetic field of the MRI scanner.[71–73] In the environment of an MRI scanner, an MHD-derived voltage overlay has been observed on traditional electrocardiograms (ECG), measures of cardiac electrical activity, known to be induced by interactions between arterial blood flow during early systole and the MRI main magnetic field (B_0).[74–76] As a large component of human blood consists of erythrocytes and a blood plasma solution of sugars, fat, proteins, and salts, human blood flow tends to be conductive,[9] causing positively and negatively charged blood particles which are flowing transversely to the strong magnetic field of the MRI scanner to be deflected by the Lorentz force, in turn inducing electrical voltages across vessel walls.[74]

These induced MHD voltages (VMHD) can often be recorded on the surface ECG inside the MRI bore, theorizing the relationship between VMHD and arterial blood flow, which has generated preliminary studies which have been able to show correlation in timing and onset between VMHD recorded on intra-MRI ECGs and MRI-derived aortic blood (**Figure 3**).[77,78]

The development of early models of the MHD effect in arterial vasculature, led to the partial validation of the hypothesis, proving that VMHD of a comparable magnitude and direction could be induced by aortic blood flow, with the primary contribution to the net signal being attributed to the aortic arch, a large diameter vasculature in the human body transverse to the MRI magnetic field and with a high volumetric flow rate.[74,79] Similarly, a phantom in vitro model was developed to record bipolar VMHD signals (**Figure 4**a) and shown to be comparable to a simplified analytical model in an MRI environment (Figure 4b), predicting a linear dependence on field strength.[80] The phantom model was constructed using rigid plastic tubing, a fluid reservoir, and a ventricular assist device, allowing the device to circulate a volume of conducting fluid while maintaining MRI-compatibility.

Dependence has been verified experimentally in human subjects by comparing directionality of induced VMHD extracted from 12-lead ECGs with the orientation of the aortic arch, illustrating an error of <3° in four human subjects.[81] In this environment, Ag/AgCl ECG electrodes are commonly used in conjunction with carbon clips and nonferrous cabling and shielding to reduce the chance for the generation of RF burns on subjects during the gradient ramps which occur during MRI scanning.[25] Similarly, a single subject was rotated on the MRI scanner table in 90° increments to illustrate the dependence of extracted VMHD on the direction of blood flow (**Figure 5**).[81] Due to the distribution of vasculature in the human body, a study sought to determine contributions to the net recorded VMHD from vasculature networks. Using MRI validation, a 1D VMHD distribution across the human body was demonstrated, showing increases in VMHD corresponding to major vasculature branches and solid organs.[82]

Despite the theorized correlation to blood flow, VMHD overlays onto surface ECGs has created difficulties in synchronizing

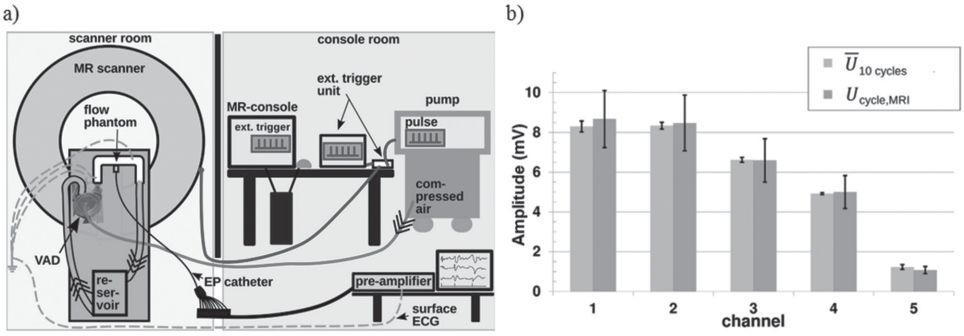

Figure 4. Development of an MHD surrogate model for the validation of induced VMHD as a blood flow potential. a) Experimental design for the recording of induced VMHD using an EP catheter located within a flow phantom. b) Comparison of MRI flow derived VMHD ($U_{10\ cycles,MRI}$) and measured VMHD ($U_{10\ cycles}$) in the flow phantom over ten cycles, illustrating flow dependence.

heart motion through its electrical activity with cardiac MRI imaging, inducing motion based artifacts onto acquisitions.[83] To increase the ability to perform cardiac synchronization during MRI imaging, customized gating and synchronization algorithms have been developed to identify the timing of ventricular contraction as marked by the QRS complex of the ECG.[83,84] Early correlation to blood flow, and therefore cardiac activity, has led to the development of VMHD driven MRI synchronization algorithms, based on the cyclic rhythm of the true QRS complex generated from the sinoatrial node and induced MHD from aortic blood flow, which allow for fine-tuning of image acquisition to better capture flow.[83–86]

5.3. Hemodynamic Measurements

Upon the examination of induced VMHD as a meaningful signal rather than a noise source which reduces accuracy in MRI synchronization,[78] and the ability to extract induced VMHD from 12-lead ECGs obtained intra-MRI,[25] came the drive to determine the clinical significance of induced VMHD. Early studies have shown the correlation of extracted VMHD with stroke volume (SV) and aortic blood flow (**Figure 6**a), illustrating a <4% error in SV estimation at rest, and a <10% error during a series of exercise stress testing (Figure 6b).[61]

The usefulness of this technique is limited to inside the MRI scanner, with an applied magnetic field of 3 T, however there are efforts to translate this technology into a stand-alone device for VMHD monitoring and potentially stroke volume or perfusion estimation.

These devices utilize conventional physiological monitoring hardware with an external neodymium magnet (grade N52), including high-impedance inputs and an embedded microcontroller for signal processing, with the major difference being in the usage of stainless steel dry electrodes rather than conventional wet Ag-AgCl electrodes (**Figure 7**a). Usefulness of the device has only been demonstrated preliminarily, and requires further validation and development to accurately predict SV (Figure 7b).

6. Conclusion

A review of the current state of the field of biomedical magnetohydrodynamics was presented, and organized to illustrate the current state of the art in three primary research areas: (1) material considerations for MHD applications; (2) MHD actuation devices; and (3) MHD sensing techniques. As magnetohydrodynamics continues to be large field of study primarily focused on macroscale interactions, increasing effort into

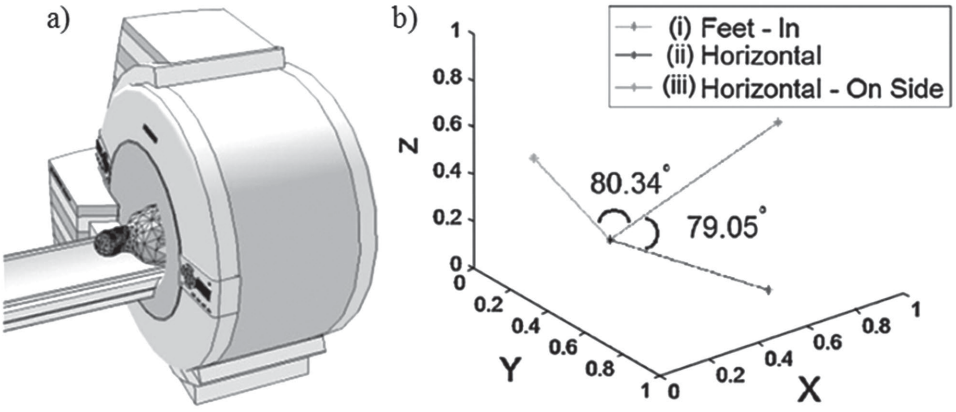

Figure 5. Assessment of dependence of induced VMHD on the direction of blood flow, achieved through subject rotation. a) Initial position of subject in the feet-in position on the scanner table. b) Extracted VMHD vectors achieved though signal time-integration, illustrating near 90° rotation.

Adv. Funct. Mater. **2015**,
DOI: 10.1002/adfm.201504198

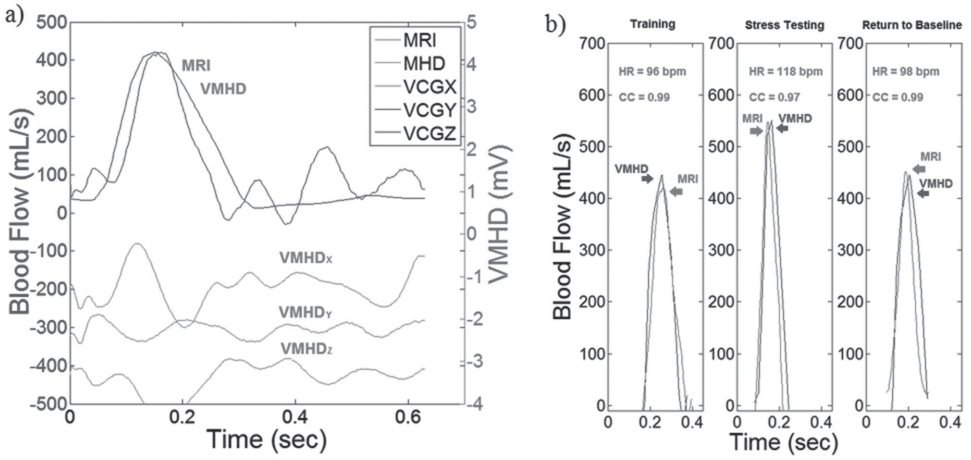

Figure 6. Aortic blood flow estimation using VMHD-derived methodology. a) MRI and VMHD derived flow (blue), compared to extracted VMHD components in the vectorcardiogram frame of reference (green). b) Comparison of beat-to-beat aortic blood flow using VMHD (blue) and MRI (red) methods.

microscale considerations and adaptions of this phenomenon is being produced, with a large attention to the growing medical field and the potential for clinical applications to expedite and increase the potential associated with current medical procedures and fields of study. The study and translation of these effects to clinical applications requires careful design considerations to be made as an effort to encourage the development of stand-alone clinical devices which can harness the MHD effect for microfluidics, particle mixing and sorting, and advanced physiological monitoring and imaging.

In order to further support the rapidly maturing field of biomedical MHDs, the growth of collaborative and interdisciplinary efforts must continue in order to meet increasing design and material constraints present in the harsh magnetic environment that may be present in MHD driven devices. These areas will revolve around sophisticated electromagnetic simulation and microelectromechanical systems (MEMS) fabrication for advanced microscale design, and further collaborative efforts as these devices aim to grow in portability and translate into clinical tools.

The efficacy of these clinical and diagnostic tools must also be examined to observe how the MHD effect could predict hemodynamics as well as how its application in medical devices may affect the human body, particularly in high-risk subjects or when the subject is placed in a large external magnetic field, which may be required for some MHD technologies. These studies may subsequently influence US Food and Drug Administration regulations regarding human magnetic field exposure and its associated effects.

Furthermore, considerations into the development of MRI-compatible and diamagnetic/paramagnetic biomaterials must be made to enable the interfacing of MHD driven medical devices with the human body, as the majority of such research has been a byproduct of conventional biomaterials research and is only recently growing into a field of research. The need for high conductivity biomaterials and composite materials, designed to capacitively couple with the human body, with limited magnetic susceptibility also presents a growing challenge to limit the external forces present on MHD actuators, drug delivery vehicles, and chemical mixers.

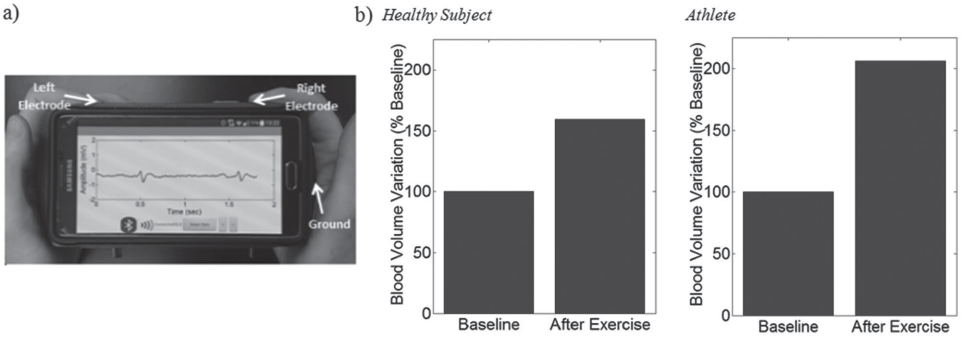

Figure 7. Development of a portable device for quantifying induced MHD voltages and estimated variations in blood flow during exercise stress testing. a) Typical usage of prototype portable flow monitoring device, illustrated during ECG acquisition. b) Time-integrated SV metrics during exercise stress testing in a normal health subject (left) and in an athlete (right).

Ultimately, while these applications of the MHD effect are technically feasible, advancement of MHD technologies should rely on a clinical need, rather than a technological push, as are the biomedical applications presented in this paper. This need will allow for the benefits of current and newly proposed MHD technologies to have a broad and real impact in scientific community and the field of medicine.

Acknowledgements

This material is based upon work supported by the National Science Foundation under Grant No. 1150042 (Rui Cheng and Leidong Mao). Research reported in this publication was also supported by the National Institute of General Medical Sciences of the National Institutes of Health under Award Numbers R21GM104528 (Leidong Mao). The content is solely the responsibility of the authors and does not necessarily represent the official views of the National Institutes of Health.

Received: October 1, 2015
Revised: November 8, 2015
Published online:

[1] E. R. Priest, *Solar Magnetohydrodynamics*, Vol. *1*, Cambridge University Press, Cambridge, UK **2003**.
[2] J. P. Freidberg, *Ideal Magnetohydrodynamics*, Plenum, New York, NY, USA **1987**.
[3] D. R. Laughlin, "*A magnetohydrodynamic angular motion sensor for anthropomorphic test device instrumentation*," SAE Technical Paper, **1989**.
[4] J. Jang, S. S. Lee, *Sens. Actuators, A* **2000**, *80*, 84.
[5] A. V. Lemoff, A. P. Lee, *Sens. Actuators, B* **2000**, *63*, 178.
[6] J. Louis, J. Lothrop, T. Brogan, *Phys. Fluids* **1964**, *7*, 362.
[7] R. J. Rosa, *Phys. Fluids* **1961**, *4*, 182.
[8] R. Blandford, K. Thorne, *Applications of Classical Physics*, CalTech, Pasadena, CA, USA **2004**.
[9] F. G. Hirsch, E. C. Texter, L. A. Wood, W. C. Ballard, F. E. Horan, I. S. Wright, C. Frey, D. Starr, *Blood* **1950**, *5*, 1017.
[10] H. H. Bau, J. Zhu, S. Qian, Y. Xiang, *Sens. Actuators, B* **2003**, *88*, 205.
[11] S. Qian, H. H. Bau, *Mech. Res. Commun.* **2009**, *36*, 10.
[12] M. Qin, H. H. Bau, *Microfluid. Nanofluid.* **2011**, *10*, 287.
[13] Y. Xiang, H. H. Bau, *Phys. Rev. E* **2003**, *68*, 016312.
[14] G. Hetsroni, A. Mosyak, E. Pogrebnyak, L. Yarin, *Int. J. Heat Mass Transfer* **2005**, *48*, 1982.
[15] N. T. Nguyen, *Microfluid. Nanofluid.* **2012**, *12*, 1.
[16] P. A. Davidson, *An Introduction to Magnetohydrodynamics*, Cambridge University Press, Cambridge, NY **2001**.
[17] J. Léorat, A. Pouquet, U. Frisch, *J. Fluid Mech.* **1981**, *104*, 419.
[18] P.-J. Wang, C.-Y. Chang, M.-L. Chang, *Biosens. Bioelectron.* **2004**, *20*, 115.
[19] H. Elhawary, A. Zivanovic, M. Rea, B. L. Davies, C. Besant, I. Young, M.U. Lamperth, *IEEE Eng. Med. Biol. Mag.* **2008**, *27*, 35.
[20] R. Gassert, R. Moser, E. Burdet, H. Bleuler, *IEEE/ASME Trans. Mechatronics* **2006**, *11*, 216.
[21] F. G. Shellock, *J. Magn. Reson. Imaging* **2002**, *16*, 485.
[22] D. Stoianovici, *Int. J. Med. Rob. Comput. Assisted Surg.* **2005**, *1*, 86.
[23] NYR Gassert, L. Dovat, O. Lambercy, Y. Ruffieux, D. Chapuis, G. Ganesh, E. Burdet, H. Bleuler, in *Proc. 2006 IEEE Int. Conf. Robotics and Automation 2006, ICRA 2006*, IEEE, New York, NY, USA **2006**, p. 3825.
[24] C. D. Wahlstrand, T. B. Hoegh, G. A. Hrdlicka, T. E. Cross Jr., J. M. Olsen, *US. Patent No.* 7,174, 219, **2007**.
[25] Z. Tse, C. L. Dumoulin, G. D. Clifford, J. Schweitzer, L. Qin, J. Oster, M. Jerosch-Herold, R. Y. Kwong, G. Michaud, W. G. Stevenson, E. J. Schmidt, *Magn. Reson. Med.* **2013**, *71*, 1336.
[26] D. F. Williams, *Definitions in Biomaterials: Proc. Consensus Conf. European Society for Biomaterials*, *1986*, Vol. *4*, Elsevier Science, Chester, England **1987**.
[27] B. D. Ratner, A. S. Hoffman, F. J. Schoen, J. E. Lemons, *Biomaterials Science: An Introduction to Materials in Medicine*, Academic, Waltham, MA, USA **2004**.
[28] J. Breme, in *Sixth World Conf. Titanium I*, Springer, Berlin, Germany **1988**, p. 57.
[29] M. Long, H. Rack, *Biomaterials* **1998**, *19*, 1621.
[30] P. Dearnley, K. Dahm, H. Çimenoğlu, *Wear* **2004**, *256*, 469.
[31] D. Velten, V. Biehl, F. Aubertin, B. Valeske, W. Possart, J. Breme, *J. Biomed. Mater. Res.* **2002**, *59*, 18.
[32] M. Khan, R. Williams, D. Williams, *Biomaterials* **1999**, *20*, 631.
[33] M. Niinomi, *Mater. Sci. Eng., A* **1998**, *243*, 231.
[34] M. F. Semlitsch, H. Weber, R. M. Streicher, R. Schön, *Biomaterials* **1992**, *13*, 781.
[35] J. West, B. Karamata, B. Lillis, J. P. Gleeson, J. Alderman, J. K. Collins, W. Lane, A. Mathewson, H. Berney, *Lab Chip* **2002**, *2*, 224.
[36] N. C. Tsai, C. Y. Sue, *Sens. Actuators, A* **2007**, *134*, 555.
[37] P. Woias, *Sens. Actuators, B* **2005**, *105*, 28.
[38] A. Homsy, S. Koster, J. C. T. Eijkel, A. van den Berg, F. Lucklum, E. Verpoorte, *Lab Chip* **2005**, *5*, 466.
[39] B. Nguyen, S. K. Kassegne, *Microfluid. Nanofluid.* **2008**, *5*, 383.
[40] S. Qian, H. H. Bau, *Phys. Fluids* **2005**, *17*, 1.
[41] N. T. Nguyen, Z. G. Wu, *J. Micromech. Microeng.* **2005**, *15*, R1.
[42] C. Y. Lee, C. L. Chang, Y. N. Wang, L. M. Fu, *Int. J. Mol. Sci.* **2011**, *12*, 3263.
[43] L. Capretto, W. Cheng, M. Hill, X. L. Zhang, *Microfluidics: Technol. Appl.* **2011**, *304*, 27.
[44] H. H. Bau, J. H. Zhong, M. Q. Yi, *Sens. Actuators, B* **2001**, *79*, 207.
[45] M. Q. Yi, S. Z. Qian, H. H. Bau, *J. Fluid Mech.* **2002**, *468*, 153.
[46] A. Affanni, G. Chiorboli, *Sens. Actuators, B* **2010**, *147*, 748.
[47] S. Qian, H. H. Bau, *Sens. Actuators, B* **2005**, *106*, 859.
[48] A. V. Lemoff, A. P. Lee, *Biomed. Microdevices* **2003**, *5*, 55.
[49] L. S. Wang, L. Flanagan, E. Monuki, N. L. Jeon, A. P. Lee, in *3rd IEEE/EMBS Special Topic Conf. Microtechnology in Medicine and Biology*, IEEE, New York, NY, USA **2005**, p. 276.
[50] T. S. Gregory, K. J. Wu, J. Yu, J. B. Box, R. Cheng, L. Mao, Z. T. H. Tse, *IEEE/ASME Trans. Mechatronics*, **2015**, *20*, 2691.
[51] J. M. Anderson, *Annu. Rev. Mater. Res.* **2001**, *31*, 81.
[52] R. Wallin, E. Arscott, *Med. Device Diagn. Ind.* **1998**, *20*, 96.
[53] S. Speakman, *U.S. Patent No. 6,164,850*, **2000**.
[54] B. C. Gross, J. L. Erkal, S. Y. Lockwood, C. Chen, D. M. Spence, *Anal. Chem.* **2014**, *86*, 3240.
[55] M. Burke, *Ph.D. Thesis*, University College London (London, UK) **2013**.
[56] G. Kósa, P. Jakab, F. Jólesz, N. Hata, in *IEEE Int. Conf. Robotics and Automation 2008, ICRA 2008*, New York, NY, USA **2008**, p. 2922.
[57] M. Simi, P. Valdastri, C. Quaglia, A. Menciassi, P. Dario, *IEEE/ASME Trans. Mechatronics* **2010**, *15*, 170.
[58] J. Bialek, A. H. Boozer, M. E. Mauel, G. A. Navratil, *Phys. Plasmas* **2001**, *8*, 2170.
[59] D. R. Laughlin, *U.S. Patent No.* 5,665,912, **1997**.
[60] A. P. Lee, A. V. Lemoff, *U.S. Patent No. 6,146,103,* **2000**.
[61] T. S. Gregory, E. J. Schmidt, S. H. Zhang, R. Y. Kwong, W. G. Stevenson, J. Oshinski, Z. T. H. Tse, *J. Cardiovasc. Magn. Reson.* **2015**, *17*, P32.
[62] K. Lurie, *Applied Optimal Control Theory of Distributed Systems*, Vol. *43* Springer Science & Business Media, Germany, Berlin, **2013**.

[63] D. R. Laughlin, *U.S. Patent No*. 5,067,351 **1991**.
[64] J. Priede, D. Buchenau, G. Gerbeth, *Magnetohydrodynamics* **2009**, *45*, 451.
[65] D. Titterton, J. L. Weston, *Strapdown Inertial Navigation Technology* Vol. *17*, IET, London, UK, **2004.**
[66] D. Eckelkamp-Baker, H. R. Sebesta, K. Burkhard, in *AeroSense 2000*, SPIE Press, WA, Bellingham, **2000**, p. 96.
[67] R. Ricou, C. Vives, *Int. J. Heat Mass Transfer* **1982**, *25*, 1579.
[68] S. Eckert, A. Cramer, G. Gerbeth, *Magnetohydrodynamics*, Springer, Berlin, Germany **2007**, p. 275.
[69] K. Fujisaki, T. Ueyama, T. Toh, M. Uehara, S. Kobayashi, *IEEE Trans. Magn.* **1998**, *34*, 2120.
[70] C. Reed, B. Picologlou, P. Dauzvardis, J. Bailey, *Fusion Sci. Technol.* **1986**, *10*, 813.
[71] D. Abi-Abdallah, V. Robin, A. Drochon, O. Fokapu, *Conf. Proc.* IEEE *Engineering in Medicine and Biology Society IEEE*, New York, NY, USA **2007**, p. 1842.
[72] T. Tenforde, C. Gaffey, B. Moyer, T. Budlnger, *Bioelectromagnetics* **1983**, *4*, 1.
[73] T. S. Tenforde, C. T. Gaffey, R. P. Liburdy, L. Levy, *Biology and Medicine Division Annual Report* Springer, Berlin, Germany **1985**, p. 66.
[74] A. Gupta, A. R. Weeks, S. M. Richie, *IEEE Trans. Biomed. Eng.* **2008**, *55*, 1890.
[75] D. Abi Abdallah, A. Drochon, V. Robin, O. Fokapu, *Eur. Phys. J. Appl. Phys.* **2009**, *45*, 11301.
[76] B. Bhatt, M. Reddy, *Ind. J. Biomech.* **2009**, 51.
[77] G. Nijm, S. Swiryn, A. Larson, A. Sahakian, *Characterization of the Magnetohydrodynamic Effect As a Signal from the Surface Electrocardiogram during Cardiac Magnetic Resonance Imaging*, IEEE, New York, NY, **2006**.
[78] G. Nijm, S. Swiryn, A. Larson, A. Sahakian, *Med. Biol. Eng. Comput.* **2008**, *46*, 729.
[79] J. Oster, R. Llinares, S. Payne, Z. T. H. Tse, E. J. Schmidt, G. D. Clifford, *Comput. Methods Biomech. Biomed. Eng.* **2015**, *18*, 1400.
[80] W. B. Buchenberg, W. Mader, G. Hoppe, R. Lorenz, M. Menza, M. Büchert, J. Timmer, B. Jung, *Magn. Reson. Med.* **2014**, *74*, 850.
[81] T. S. Gregory, E. J. Schmidt, S. H. Zhang, R. Y. Kwong, W. G. Stevenson, J. R. Murrow, Z.T.H. Tse, *Ann. Biomed. Eng.* **2014**, *42*, 2480.
[82] T. S. Gregory, E. J. Schmidt, S. H. Zhang, J. R. Murrow, T. T. Zion, *Circulation* **2014**, *130*, Suppl 2.
[83] T. S. Gregory, E. J. Schmidt, S. H. Zhang, Z. T. H. Tse, *Magn. Reson. Med.* **2014**, *71*, 1374.
[84] S. E. Fischer, S. A. Wickline, C. H. Lorenz, *Magn. Reson. Med.* **1999**, *42*, 361.
[85] T. Frauenrath, M. Dieringer, N. Patel, C. Ozerdem, U. Hentschel, W. Renz, T. Niendorf, *Proc. Int. Soc. Mag. Reson. Med.* **2011**, 19.
[86] T. Frauenrath, K. Fuchs, M. Dieringer, C. Ozerdem, N. Patel, W. Renz, T. Niendorf, *J. Magn. Reson. Imaging* **2012**, *36*, 364.
[87] R. Langer, N. Peppas, *Biomaterials* **1981**, *2*, 201.
[88] L. S. Nair, C. T. Laurencin, *Prog. Polym. Sci.* **2007**, *32*, 762.
[89] X. Kang, Z. Mai, X. Zou, P. Cai, J. Mo, *Anal. Biochem.* **2007**, *363*, 143.
[90] T. Chandy, G. S. Das, R. F. Wilson, G. H. Rao, *Biomaterials* **2000**, *21*, 699.
[91] B. D. Ratner, *Biomaterials* **2007**, *28*, 5144.
[92] R. A. White, *ASAIO J.* **1988**, *34*, 95.
[93] W. Czaja, A. Krystynowicz, S. Bielecki, R. M. Brown, *Biomaterials* **2006**, *27*, 145.
[94] A. Hou, M. Zhou, X. Wang, *Carbohydr. Polym.* **2009**, *75*, 328.
[95] M. F. Refojo, *Surv. Ophthalmol.* **1982**, *26*, 257.
[96] A. Kotwal, C. E. Schmidt, *Biomaterials* **2001**, *22*, 1055.
[97] L. Robblee, J. McHardy, J. Marston, S. Brummer, *Biomaterials* **1980**, *1*, 135.
[98] M. Yang, F. Qu, Y. Lu, Y. He, G. Shen, R. Yu, *Biomaterials* **2006**, *27*, 5944.
[99] M. P. Staiger, A. M. Pietak, J. Huadmai, G. Dias, *Biomaterials* **2006**, *27*, 1728.
[100] F. Witte, N. Hort, C. Vogt, S. Cohen, K. U. Kainer, R. Willumeit, F. Feyerabend, *Curr. Opin. Solid State Mater. Sci.* **2008**, *12*, 63.